A STUDY OF SECOND HARMONIC EMISSION FOR CHARACTERISATION OF LASER PLASMA X-RAY SOURCES

A. Giulietti, C. Beneduce, T. Ceccotti[1], D. Giulietti[2], L.A. Gizzi And R. Mildren

Istituto di Fisica Atomica e Molecolare, Via del Giardino , 7 , 56127 Pisa, Italy
[1]*presently at Universitè Paris VI, France*
[2]*also at Dipartimento di Fisica, Università di Pisa, Italy*

ABSTRACT

An investigation of both second harmonic (SH) and X-ray emission from Al plasmas produced by 3 ns, 1.064 μm, laser pulses at 10^{14}W/cm^2 is reported. The SH and the X-ray yield are strongly correlated as a function of the target position with respect to the laser beam focus. SH is found to originate from the underdense coronal plasma and to have a filamentary source, while the X-ray source is uniform. The results suggest that, though X-ray emission is significantly enhanced by filamentation of the laser light in the corona, there is a *smoothing* effect in the energy transport process towards the overdense region.

1. Introduction

At temperatures of hundreds eV, typical of laser produced plasmas (LPP), the energy emitted in the X-ray region of the spectrum is a relevant percentage of the absorbed laser energy. While the laser energy is absorbed in the underdense plasma ($n_e < n_C$, where $n_C = m \omega^2 / 4 \pi e^2$ is the critical density for e.m. radiation of angular frequency ω), most of the X-ray emission is generated in the overdense region. Thus the study of energy transport from the underdense to the dense region of the plasma is relevant to both basic plasma physics and optimisation of laser produced X-ray sources. It is well known that the X-ray conversion efficiency increases using shorter laser wavelengths, in order to keep the absoption region close to the X-ray emitting layer. However investigations with near-infrared lasers are relevant for two distict reasons: i) many practical X-ray sources are operating in this regime; ii) in this condition the laser-plasma interaction region is well decoupled from the main X-ray generating layers, allowing more accurate measurements on the effects related to each region, as well as on their interplay. In addition, due to the lower threshold intensities for non-linear processes,

longer wavelength laser light gives rise to more efficient production of hot electrons and therefore to brighter X-ray emission in the harder (≈10keV) region.

A recent experiment (Macchi et al. 1996) with 1 μm laser light suggested that the X-ray conversion efficiency is enhanced by the filamentation instability (FI). A useful diagnostic to study the FI is supplied by second harmonic (SH) emission. In fact, SH emission sources are localised into density and intensity inhomogeneities (Stamper et al. 1986, Schifano et al. 1994). Previous measurements (Biancalana et al. 1993) based on SH emission have indeed shown that the FI causes the laser beam to break into several beamlets due to a positive feedback between laser hot spots and channels in the electron density (Sodha et al. 1976).

All these experiments demonstrate that simultaneous measurements of SH and X-ray emission provide invaluable information on the physics of laser interaction with plasmas. This method was recently used also for the study of X-ray emission from ultrashort pulse laser irradiation of solid targets (Gizzi et al, 1996), showing also in that case very interesting correlations in spite of the deeply different interaction regime.

In this paper we report on an investigation of both second harmonic and X-ray emission from a plasma produced by a 3 ns, 10^{14}W/cm^2 laser pulse focused on a massive aluminium target. SH and X-ray emission were studied as a function of the target position with respect to the laser beam focus. Imaging techniques were used to analyse the structure of SH and X-ray sources. Finally, time resolved analysis of SH emission and $3\omega/2$ was also carried out. The experimental set-up is described in Sect.2, while results are presented and discussed in Sect.3.

2. Experimental set-up

The experimental set-up is shown in **Fig 1**. A Nd laser (λ = 1.064 μm) delivering 1.5J on target in 3 ns pulses was used. Laser energy, pulse shape, and focal spot were monitored shot by shot by using a fast photodiode, a calorimeter, and an equivalent plane CCD, respectively. The focal spot was measured to be 24μm in diameter. The laser operated in a single transverse, multiple longitudinal mode. Consequently the laser emission was strongly modulated in time by non-reproducible spikes whose mean duration was measured to be about 50 ps, as expected from mode beating in the oscillator cavity.

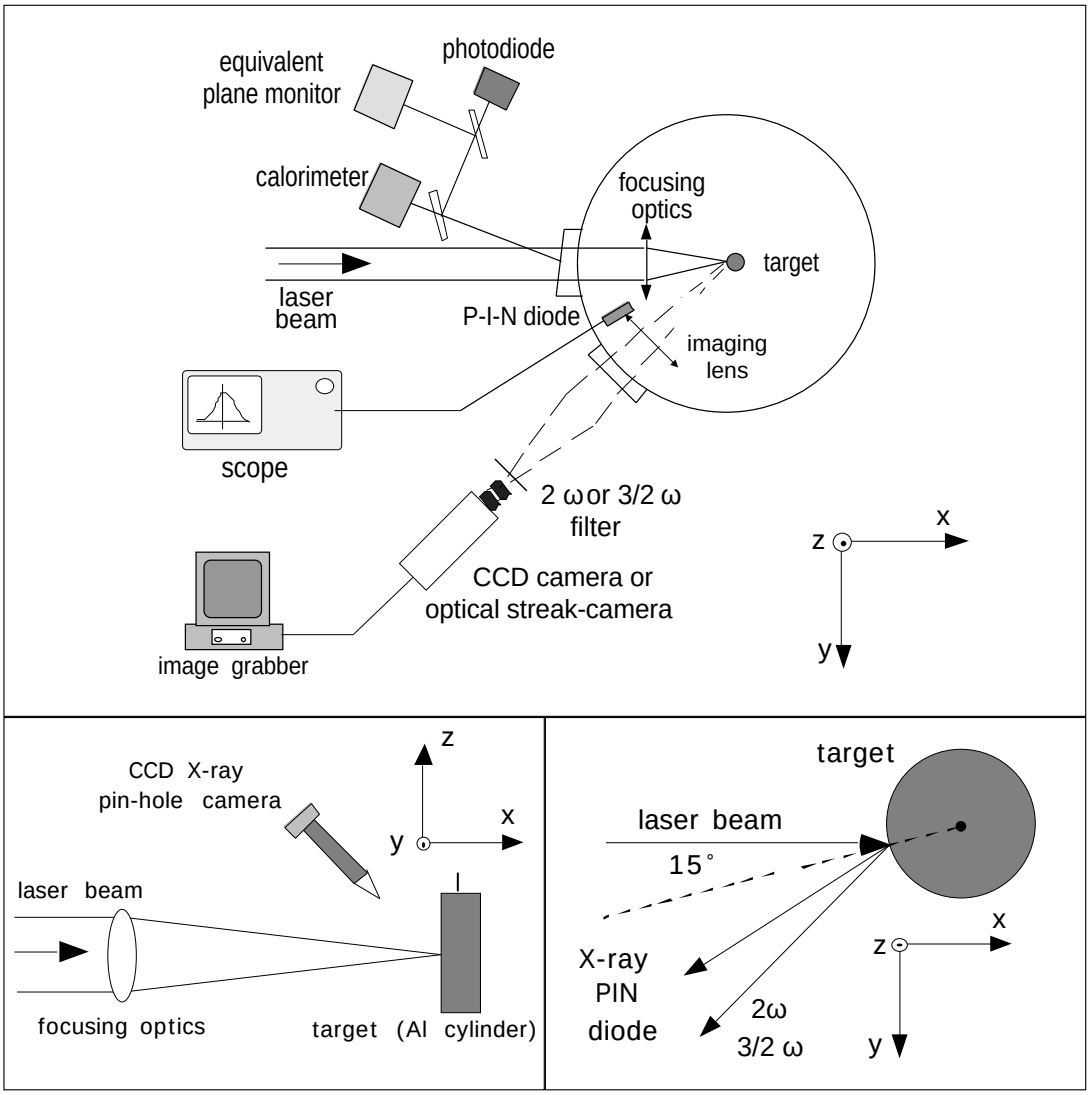

Fig.1: Layout of the experimental set-up. In the separate boxes are shown: i) the pin-hole camera setting; ii) the geometry of laser incidence and radiation emission detection.

The laser beam was focused on target by an f/8 optics at an incidence angle of 15 deg so as to avoid back reflections. The FWHM spot size without plasma was mesured by equivalent plane monitor and was found to be approximately 24 μm. Therefore, the nominal irradiance on the target of about 10^{14} W/cm^2.

The X-ray emission was detected at 30 deg from the laser beam axis, by using an X-ray P-I-N diode, filtered by a 8 μm Beryllium foil. Taking into account the transmittivity of the Beryllium filter and the spectral sensitivity of the P-I-N diode, the investigated X-ray spectral region was in the 1-10keV range, with its maximum at ≈1.7keV. Time-integrated images of the X-ray source were taken by using an CCD pin-hole camera (set as shown in Fig1b) filtered with a 8 μm Beryllium foil. The spatial resolution, determined by the pin-hole size, was 13 μm.

The SH radiation emitted at 45 deg was collected by an f/5 optics and analysed in different ways. Firstly, time-integrated images of the plasma were formed on a CCD after passing through a narrow-band (≈30 Å) interference filter centred at ≈5320 Å. The resolution of the imaging optics was estimated to be of the order of 10 μm. Secondly, a fraction of the SH light was sent to a photomultiplier to measure the amplitude of the SH signal. Thirdly, time-resolved SH images of the plasma were formed directly on the slit of an optical streak camera to perform 1-D time resolved imaging. Alternalively, an optical spectrometer was coupled to the streak camera to perform time resolved spectroscopy of SH emission with a spectral resolution of ≈ 2 Å. The same measurements were also performed on 3ω/2 emission by using an interference filter centred at ≈7060 Å.

3. The experimental results

3.1 X-ray and SH yield measurements

The two plots of Fig. 2 show X-ray and SH intensity as a function of the target position with respect to the laser beam focal plane (x =0) with x increasing in the direction of propagation of the laser beam. The position of the focal plane was determined with an uncertainty of ± 200 μm. Both SH and X-ray emission intensities vary considerably when moving the target within a ± 2 mm range from the focal plane; both intensities are found to be minimum for zero target position and show maxima between -1 and -0.5 mm on one side and 0.5 on the opposite side. A similar behaviour was already observed in previous measurements on SH emission (Biancalana et al.1993); in that work, a strong correlation between SH generation and the onset of filamentation was experimentally proved. The present measurements provide evidence of a strong correlation between SH and soft-X-ray emission

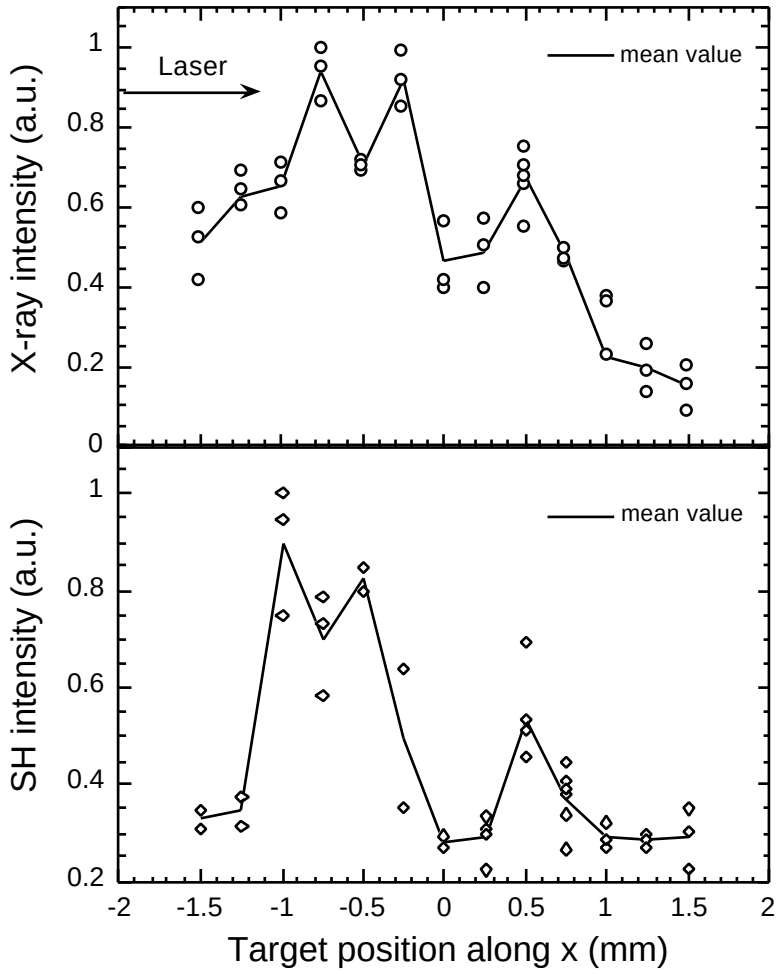

Fig.2: X-ray (top) and Second Harmonic (bottom) intensity as a function of the target position with respect to the laser beam focal plane

3.2 Identification of SH sources

The sources of SH emission have been localised by using two different techniques based upon imaging and spectroscopic measurements, respectively.

Firstly, the plasma was imaged at 45 deg with respect to the beam axis (i.e. 30 deg from the plasma expansion axis) in both 2ω and $3\omega/2$ light on the slit of the optical streak-camera. The slit was set to select a given slice of the image in order to investigate the corresponding plasma region. Fig.3 shows the streak images of three different regions in 2ω and $3\omega/2$ light. Both 2ω and $3\omega/2$ show a spiky structure in time with a poor shot-by-shot reproducibility. Fig.3 clearly shows that the overall intensity of $3\omega/2$ emission decreases strongly as plasma

regions farther from the target are selected. We recall that $3\omega/2$ harmonic emission is a signature of the $n_c/4$ electron density layer in the plasma (Giulietti D. et al. 1993).

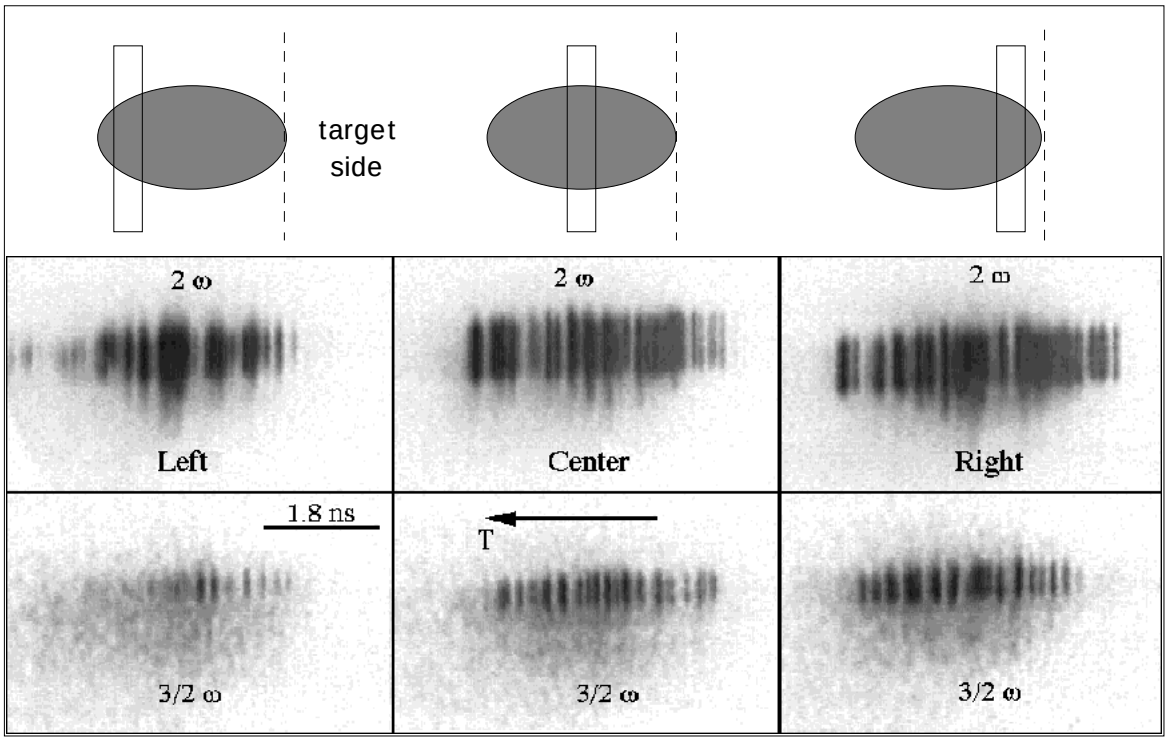

Fig.3: Time-resolved (streaked) images in 2ω and 3ω/2 light of three different regions of the plasma.

Such a dramatic reduction in the intensity is not observed in the case of SH emission.. Moreover, SH radiation is emitted from a broader plasma region than the $3\omega/2$ radiation. Once the line of view of the detector is taken into account, these observations show that i) the region from which SH is originates is wider than the $3\omega/2$ emitting layer ($\approx n_c/4$); ii) the SH emitting region is characterised by an electron density less than $n_c/4$.

Another measurement consisted in time-resolved spectroscopy of the SH emission. All the time-resolved spectra showed that the emitted SH radiation was found to be shifted from the exact $2\omega_0$ frequency, and broadened in comparison with the width of the purely frequency doubled radiation. A typical time resolved spectrum is shown in Fig.4. Such spectra were interpreted in terms of the theory introduced by Stamper et al.(1985) and experimentally proved (Giulietti A. et al. 1989). According to this theory, the generation of substantial SH emission in filamentary plasmas requires the existence of either a reflected or a stimulated Brillouin backscattered (SBS) wave within the filament.

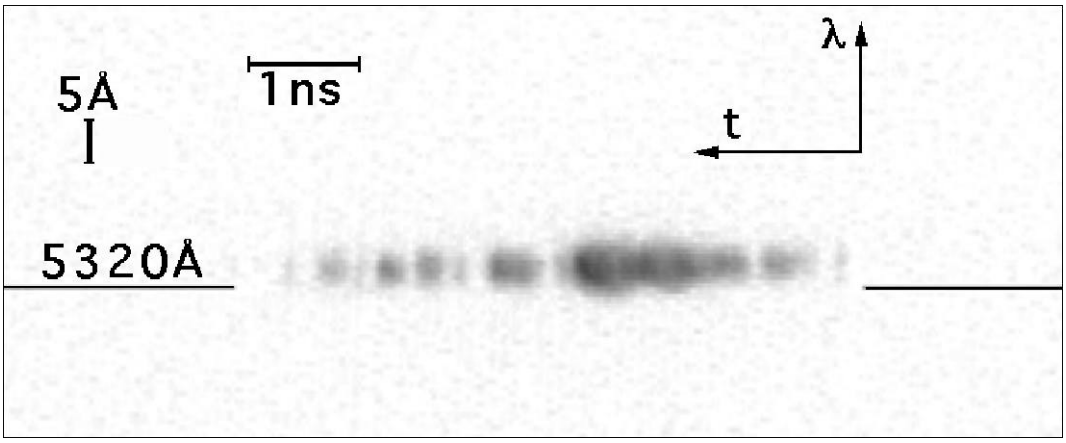

Fig.4: Time-resolved Second Harmonic spectrum. The horizontal lines indicate the calibrated position for the 5320 Å wavelength.

For backward emitted SH (which is close to our experimental condition) the frequency of the SH radiation is $\omega_b+\omega_b$, where ω_b is the frequency of the Brillouin backscattered wave and the shift can be written as:

$$\left(\frac{\Delta\omega}{\omega}\right)_{2\omega_0} = \left(\frac{\Delta\omega}{\omega}\right)_{\omega_0} \approx \frac{2}{c}\left(v_S + v_p\right) \qquad (1)$$

where v_S = 1.5 10^7 *cm/s* is the speed of the ion-acoustic wave (assuming T_e = 500 *eV*) and v_p is the flow velocity of the plasma. Using equation (1), from the observed spectral shift we obtain 9.4 10^6 *cm/s* <v_p<1.9 10^7 *cm/s*. By comparing the values of the flow velocity obtained from the SH spectra with the hydrodynamic simulations of the 1-D hydrocode MEDUSA (Christiansen et al. 1974, Rodgers et al. 1989), the region of dominant SH emission can be then located at 80 μm from the critical layer, where the electron density ranges between 1.4 and 2.0 10^{20} *cm* $^{-3}$. These values must be considered only as an estimate of the order of magnitude, because of the limits of applicability of the simulation code set by the 1-D approximation for the plasma motion. In fact, the 1-D approximation leads to underestimating the adiabatic cooling of the plasma during expansion, as well as overestimating the density scalelength and the consequent laser energy absorption. However, since the simulation is likely to overestimate both density and velocity in a given point in space, these values give an upper limit to the density of the SH emitting region. Thus we conclude that SH emission definitely comes from a region with a density below $n_c/4$, in agreement with the result previously obtained from the comparison of the 2ω and 3ω/2 images.

How the intense Brillouin backscattering required by our model may be activated, is an interesting question. Considering that SH emission is observed in the region with $n_c/ < n_c/4$, an attractive hypothesis is that SBS would be enhanced there by stimulated Raman Scattering (SRS) via decay process of the SRS driven plasma wave. In this case SH could be the signature of SRS, via SRS-enhanced SBS in filaments, rather than non-enhanced SBS in filaments. In this scenario filaments may also extend beyond the $n_c/4$ layer. In what concerns the spiky behaviour, which is already present in the laser pulse, it may be accentuated by the typical temporal modulation of the filaments themselves in the nonlinear regime of filamentation and/or by the interplay between filamentation and SBS.

3.3 Intensity distribution

In this section we compare X-ray plasma images obtained by the pin-hole camera, with images of the plasma in SH light. X-ray images taken for different target positions ($-500 < x < +500$ μm) along the laser beam propagation axis show that the shape of the X-ray emitting region does not vary significantly. In contrast, the shape of the SH emitting region is found to change even for a small target displacement. The latter observation is consistent with previous measurements (Biancalana et al., 1993). These images are also compared with the intensity distribution of the laser spot without plasma, shown in Fig.5a, as obtained by equivalent plane imaging. The measured FWHM spot size was 24 μm, and the intensity distribution in the spot was found to be rather uniform within the resolution of ≈ 4 μm.

A SH image, taken with the target in the position $x = 0$, is shown in Fig.5b. The SH emission from the corona shows structures with a typical size of 10-20 μm. It is interesting to compare this scalelength with the sclelength of maximum growth for the filamentation instability in our plasma conditions. A detailed analysis would require a sophisticate simulation of non-stationary (possibly nonlinear) filamentation which is beyond the aim of this work. Here we only give an estimate based upon a detailed kinetic theory of thermal filamentation (Epperlein 1990).

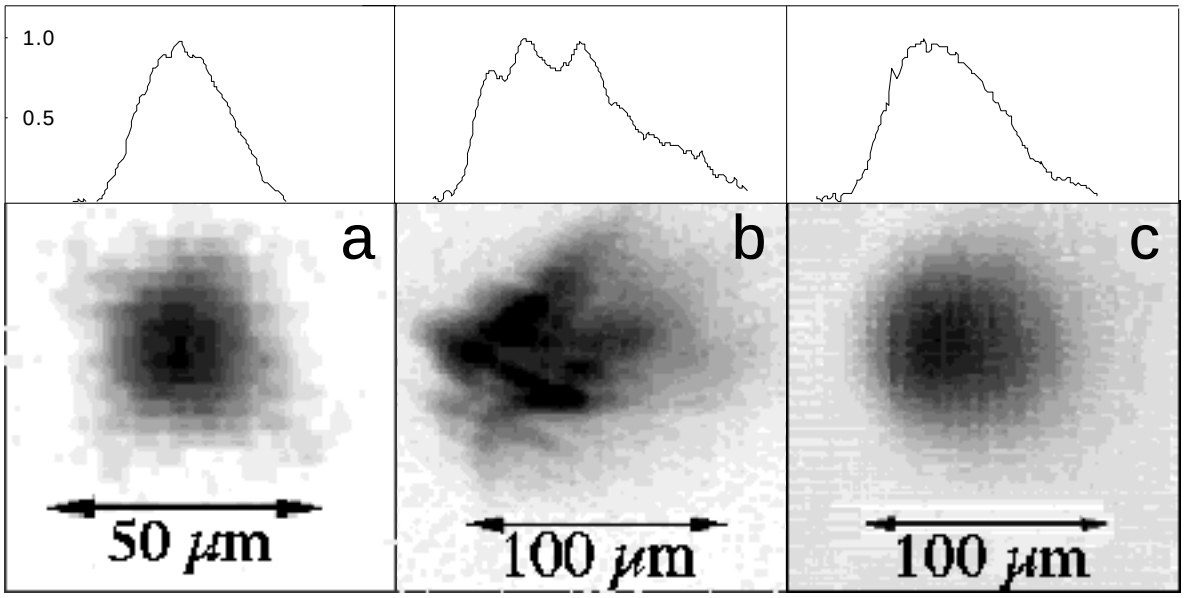

Fig.5: Images showing the intensity distribution and the corresponding lineouts for a) the 1.06 μm wavelength laser focal spot; b) the Second Harmonic source; c) the X-ray source.

According to this theory, the maximum growth rate, K_{max} and the optimum perturbation wavelength, λ_{max} are given by:

$$K_{\max} = 2\ 10^{-2}\,\mu m^{-1}\ \frac{Z\ I_L^{3/4}\left(n_e/n_c\right)^{5/4}\left(\ln\Lambda\right)^{1/2}}{\varepsilon^{7/8}\ T^{7/4}\ \phi^{7/4}\left(1+1/Z\right)^{1/2}}$$

$$\lambda_{\max} = 15\ \mu m\ \ \frac{\varepsilon^{3/16}\ \lambda_L^{1/2}\ T^{7/8}\ \phi^{3/8}\left(1+1/Z\right)^{1/4}}{I_L^{3/8}\left(n_e/n_c\right)^{5/8}\left(\ln\Lambda\right)^{1/4}} \qquad (2)$$

where $\phi=(Z+0.24)/(1+0.24Z)$, I_L is the laser intensity in units of 10^{14} Wcm^2, λ_L is the laser wavelength in μm, T is the electron temperature in keV, $\ln\Lambda$ is the Coulomb logarithm and ε is the plasma dielectric constant. Assuming $T \approx 0.5$ keV, $I_L \approx 10^{14}$ Wcm^{-2} , $(n_e/n_c) \approx 10^{-1}$, we find, from the relations (2), $K_{max} \approx 5\ 10^{-3}$ μm^{-1} and $\lambda_{max} \approx 10$ μm. The estimated growth rate is consistent with the focal depth of our focusing optics and the optimum perturbation wavelength agrees with the observed perturbation scalelength**.**

Finally, Fig.5c shows an X-ray pin-hole camera image of the plasma, with a resolution of 13 μm. In the limit of such a resolution, the X-ray emitting region is uniform, in spite of the filamentary distribution of SH emission in the corona.

A qualitative explanation for this result can be given by comparing the typical size of the inhomogeneities in SH emission with the mean free path of thermal electrons λ_e. According to the classical theory of thermal diffusion (Spitzer & Harm 1953) we have

$$\lambda_e \quad 1.5\ 10^{13} cm \frac{T_e^2}{Z n_e \ln\Lambda} \qquad (3)$$

where T_e is in eV. Therefore λ_e is found to range between 10 and 10^2 μm in the corona ($n_e \approx 10^{20}$ to 10^{21} cm^{-3}). Hence, any spatial inhomogeneity, with a typical scale of 10 μm or less, in the distribution of laser energy deposition in the corona will be "smoothed" out during the thermal energy transport towards the overdense region. However, it should be noted that the classical theory of thermal transport (which holds for plasmas produced by quite long, moderate intensity laser pulses as in the present case) may become invalid if local sharp density gradients are generated by the onset of FI. Thus the detailed mechanisms of thermal energy transfer from the corona to the denser plasma region should require a more detailed theoretical description.

4. Conclusion

Second Harmonic emission was used as main diagnostic of the laser-plasma interaction in a laser generated plasma X-ray source. SH intensity mesurements and source imaging were proved to be effective tools to investigate a regime (1.06 μm, 3 ns, 10^{14} Wcm^{-2}, Al target) dominated by filamentation. Simultaneous measurements of SH and X-ray emissions for different positions of the target showed a strong correlation between the two emissions, with the evidence that a higher level of filamentation corresponds to an increased laser-to-X-ray conversion efficiency. The region in which SH generation (and hence filamentation) takes place was identified into the underdense corona, far from the overdense X-ray emitting region. The SH source was found to be divided in filaments, whose structure is very sensitive to the target position. On the contrary, the soft X-ray source was found to be rather smooth, and its uniformity was surprisingly almost unaffected by target displacements as large as several Rayleigh lengths of the focusing optics. This is consistent with previous observations showing

that the dependence of the X-ray yield upon target position is not due to a purely geometrical effect. Moreover there is here an interesting evidence of a smoothing effect operated by the energy transport process from the coronal filamentary region to the dense plasma. Our study shows that a filamentary regime of laser-plasma interaction may be suitable for the production of a rather efficient, smooth source of soft X-rays.

References

BIANCALANA, V. *et al,* 1993 *Europhys. Lett.*, **22**, 175.

CHRISTIANSEN, S.P., *et al,* 1974 *Comp. Phys. Comm.* **7**, 271.

EPPERLEIN, E.M., 1990 *Phys. Rev. Lett.,* **65**, 2145.

GIULIETTI, A. *et al,* 1989 *Phys. Rev. Lett.,* **63**, 524.

GIULIETTI, D. *et al,* 1991 *Il Nuovo Cimento D,* **13**, 845.

GIZZI L.A. *et al,* 1996 *Phys. Rev. Lett.,* **76**, 2278.

MACCHI, A. *et al,* 1996 *Il Nuovo Cimento D,* **18**, 727.

RODGERS, P.A., *et al,* 1989 RAL report No. RAL-89-127 , unpublished.

SCHIFANO, E., *et al,* 1994 *Las. Part. Beams* **12**, 435.

SODHA, M.S., *et al* , 1979 *Progress in Optics* **13**, 171.

SPITZER, L. & HARM, R. 1953 *Phys. Rev.,* **89**, 977.

STAMPER, J.A. *et al,* 1985 *Phys.Fluids,* **28**, 2563.